Mapping tree root system in dikes using induced polarization: Focus on the influence of soil water content

Benjamin Mary, Ginette Saracco, Laurent Peyras, Michel Vennetier, Patrice Meriaux, Christian Camerlynck

http://dx.doi.org/10.1016/j.jappgeo.2016.05.005

Journal of Applied Geophysics, 135, 387-396, 2016

Mapping tree root system in dikes using induced polarization: Focus on the influence of soil water content

Benjamin Mary [a,b,*], Ginette Saracco [b,d], Laurent Peyras [a], Michel Vennetier [a,d], Patrice Mériaux [a], Christian Camerlynck [c]

[a] Irstea, UR RECOVER, 3275 route de Cézanne, Aix-en-Provence, France
[b] CNRS–UMR7330, CEREGE, AMU, Equipe Modelisation, Europole de l'Arbois, BP80, F-13545 Aix-en-Provence-cedex4, France
[c] Sorbonne Universités, UPMC Univ Paris 06, UMR 7619 METIS, Paris, France
[d] ECCOREV FR 3098, Université Aix-Marseille, France

Article history:
Received 30 April 2015
Received in revised form 29 April 2016
Accepted 18 May 2016
Available online 19 May 2016

Keywords:
Embankment hydraulic structures
Electrical prospecting
Root detection
Soil moisture
Induced polarization (IP)

Article abstract

In this study, we assessed induced polarization as potential non-destructive method for root detection in dike embankments. We used both laboratory and field experiment to describe the electrical signal with a focus on soil water content. Our objective was to determine in which hydric state of the soil, and related electrical properties, roots could be accurately discriminated. We hypothesized that preferential water zone absorption near the roots could, in some conditions, contribute to locate them.

During the laboratory experiments, we compared the response of containers filled with the same homogeneous silty clay bare material, and without (A) or with freshly cut root (B) at different levels of soil water content. Resistivity and phase variations with soil water content indicated that it was preferable to work in dry conditions since the contrast was higher.

Interactions and overlapping between polarization effects of both root and soil made it difficult to interpret first chargeability maps. This led us to study temporal-spatial variations by considering the dynamics of water absorption during a field experiment.

High resolution time lapses images showed a correlation between root location and complex resistivity anomalies. Although these first results have to be confirmed by further measurements, induced polarization seems to add useful information to interpret anomalies produced by woody roots.

1. Introduction

1.1. Context and background

Controlling the vulnerability of dike embankment is one of the main concerns for river managers. A regular monitoring and diagnosis is necessary. Indeed, the failure of such dikes may have catastrophic socio-economic impacts including casualties for neighboring populations. In the world, tens of thousands of kilometers of dikes were insufficiently maintained in the past (Sharp et al, 2013; Zanetti et al, 2011a, 2011b) and sometimes planted with trees, leading to the development of woody vegetation on these embankments and their surroundings. Tree rooting in dikes generates significant risks, particularly a risk of internal and external erosion (Patrice Mériaux et al., 2006). Internal erosion by piping occurs when particles are torn off and transported along preferential pathways and is one of the main causes of dike failure (Foster et al., 2000). It can be initiated by the presence of root systems that constitutes areas of heterogeneities particularly with root decay (Bambara et al., 2013) after tree death or coppicing. Information on the soil type is useful to assess the behavior of the pipe after root decomposition. The more the soil material is cohesive, the longer the root way is preserved (Deroo and Fry, 2014). Dikes which material is in majority fine (silt and clay) as they generally have to be impermeable, are therefore vulnerable to root decay. External erosion (slopes and crest) is often related to trees blown over. Recent work by Vennetier et al. (2015) and Zanetti et al. (2015) allowed understanding the way tree root systems and more specifically large roots develop in dikes: they showed that this development depends on environmental conditions such as material type, water-table level and climate as well as tree position on the embankment. They related root system types and the architecture of individual roots to these conditions. This helps river managers to assess the level of risk related to these trees depending on their location and their age. Nevertheless uncertainties remain especially when the nature and spatial distribution of the materials are unknown.

* Corresponding author at: Irstea, UR RECOVER, 3275 route de Cézanne, Aix-en-Provence, France.
E-mail addresses: benjamin.mary@irstea.fr (B. Mary), saracco@cerege.fr (G. Saracco), laurent.peyras@irstea.fr (L. Peyras), michel.vennetier@irstea.fr (M. Vennetier), patrice.meriaux@irstea.fr (P. Mériaux), christian.camerlynck@upmc.fr (C. Camerlynck).

Moreover neither the position of individual roots nor their size can be accurately determined. To date, only a careful extraction of tree root system allows checking this information, which is very expensive, binding in terms of security and sometimes impossible without a full renovation of the dike. Research programs offer strands on the contribution of geophysical methods applied to hydraulic structures (Corcoran et al., 2010). Geophysical methods are commonly used to explore soil heterogeneities, nevertheless, given the complex variety of soil properties composing earth dikes, these non-destructive methods have to be adapted and improved in order to obtain an accurate but cheaper map of coarse roots.

1.2. Geoelectrical methods for root tomography: background and limitations

1.2.1. Potential pitfalls of classical electrical resistivity tomography

Up to now, the electrical method has been used widely especially for the study of root biomass (Amato et al., 2008, 2009). Basically the use of a classical electrical resistivity tomography (ERT) provides an approximation of the distribution and the volume of the root system. This constitutes a first limit to be tackled because in this case the resolution is not high enough to discriminate individual dangerous roots.

Recently, Mancuso (2011) and Vanderborght et al. (2013) proposed an overview of the methods used for studying root zone properties. They pointed out many gaps and challenges of the electrical approach. Among the limits underlined, the main is that the classical electrical tomography is an indirect determination of the presence of roots. Indeed, in some cases, the ranges of electrical resistivity of soil and roots overlap. First, the range of electrical resistivity of roots depends on their nature (Amato et al., 2009; Zenone et al., 2008). Typically coarse roots, due to the effect of dead wood (heartwood) and the isolative layer of bark appear more resistive compared to fine roots (Hagrey and Michaelsen, 2002; al Hagrey, 2007). Electrical resistivity is also linked to the physiological state of the roots. Depending on the season, roots carry more or less electrical charges as sap composition is variable and sap flows vary in intensity and direction. Wood composition and physical properties also change with root decay which implies a variation of electrical properties (Martin and Günther, 2013; Martin, 2012, 2009; Weller et al., 2006). Finally, water uptake from the soil by root activity and the release of different exudates by fine roots change soil water content and resistivity at several temporal scales: on a daily basis (night vs day, sunny vs cloudy days) and seasonally (growth period vs winter or drought season). Both roots and soil parameters act on the variations and the range of electrical resistivity.

1.2.2. Extension to induced polarization to prospect for roots.

A promising approach for localizing more accurately root systems is to consider the induced polarization (IP) method. Related to the classical ERT, this method includes a temporal dimension and allows assessing an additional physics called polarization (Kemna et al., 2000). The temporal dimension is linked to the time dependency of the response of a material following the stimulation by an electrical alternative field. The analogy with an electrical capacitor which stores and restitutes electrical energy over time is common, particularly for root response modeling (Aulen and Shipley, 2012; Gurin et al., 2013; Preston et al., 2004). Any material is polarized on the passage of an alternative electric field. So IP effect should be observed in the presence of organic material. Plant and root materials are expected to polarize stronger than the soil in the presence of an alternating electrical field (J. Vanderborght et al., 2013). According to Weller et al. (2006) and (Thierry et al., 2001) the polarization effect in wood is caused by differences in the mobility of ions through cell membranes and results in a separation of charge carriers of different polarity. Zanetti et al. (2011a, 2011b) has confirmed by investigations of different types of wood that the porous structure causes remarkable polarization effects. Beyond the polarizing power of the root, the mechanisms of polarization of a biological material potentially allow us to obtain a specific signature necessary for soil discrimination. The studies led by Martin (2012) and Schleifer et al. (2002) respectively on living tree stems and an archeological plankway reported the successful application of SIP (spectral induced polarization) where IP effects were observed. These effects were all identified at frequencies bellow 10^2 Hz. The ability to detect a root depends also on the type of the surrounding soil. The higher the contrast of electrical properties between soil and roots, the easier the discrimination. According to existing literature and especially to Zanetti et al. (2011a, 2011b), gravel and sand provide better conditions for root detection using induced polarization than silt and clay which seem closer to root samples in term of electrical properties.

1.3. Contribution of the water content in root zone

Among the parameters controlling the ability to detect roots with IP methods, water content of the soil seems preponderant since it affects the contrast of conductivity between soil and root. Water content relation with electrical resistivity of the soil is known by some descriptive law as Archie's Law (Archie, 1942). Typically a non-linear increase of the amplitude of resistivity is observed when the soil water content decreases. Physically this is understood as the decrease in available carried charges. Therefore variations in soil water content may sometimes explain more variance in electrical resistivity than roots, and the effect of woody roots should be detectable only if the root mass density is high enough. Moreover electrical tomography is able to resolve targets and structures (in 2D/3D) and monitor water processes (with additionally a temporal dimension). Living trees interact with the environment to access resources and root water uptake occurs at roots-soil interface (Nadezhdina et al., 2008). The integration of induced polarization effects could be a real asset to the location of the roots via the dynamics of water absorption. The study conducted on large-leaved lupine (*Lupinus polyphyllus*) by Werban et al. (2008) provides an example of roots mapping using the resistivity method before and after irrigation. This study, however, only investigated the classical resistivity.

The main objective of this paper is to determine whether induced polarization brings useful additional information for the identification of root anomaly in the soil. We hypothesized that, both soil and biological material respond to polarization effects, but that this response could be different according to soil properties, particularly water content, which may allow the identification and mapping of anomalies related to the presence of roots.

2. Material and method

During the experiments, we choose to work with only one type of soil, a sandy and clayey silt representative of the material of many dikes. The granulometry, determined according to the NF P 94-056 and NF P 94-057 norms, respectively for screening and sedimentation, is described in Table 1. Also, we only investigated the ability of the method to detect large woody roots (≥5 cm), the most dangerous for dikes.

In this section, we present successively: in Section 2.1, the IP method used; in Section 2.2, a laboratory study on water-content-dependent IP properties of the material with and without buried root samples suggesting the most favorable conditions of both current frequency and water content for the discrimination between soil and roots, to be

Table 1
Soil grain size distribution.

<2 μm	Clay	22.7%
2 μm–50 μm	Silt	51.6%
50 μm–2 mm	Sand	19.2%
2 mm–100 mm	Gravel	5.8%

used in the field; in Section 2.3, the methodology adopted for the field study.

2.1. Induced polarization and physical quantities measured

A survey by induced polarization is performed using an equipment injecting, with two electrodes, a source of alternative current into the soil. The measure of the resulting electric field E is carried out through two other electrodes. To describe the electrical properties of a material, we refer to the concept of resistivity (ρ) or its inverse, the conductivity (σ). Conductivity is directly related to the Ohm's law written under complex form from Maxwell's equations.

$$\text{Ohm's Law } \vec{j}^{*}(\omega) = \sigma^{*}(\omega)\vec{E} \tag{1}$$

Conductivity is written as a complex quantity (Eq.Eq. 2) to describe both the effects of conduction and polarization (Olhoeft, 1985; Weller et al., 2000) where ω is the angular frequency.

$$\sigma^{*}(\omega) = |\sigma(\omega)|e^{j\varphi(\omega)} = \sigma'(\omega) + i\sigma''(\omega) \tag{2}$$

$$\rho^{*}(\omega) = \frac{1}{\sigma^{*}(\omega)} \tag{3}$$

i is the imaginary unit.

Both the real (σ') and the imaginary (σ'') parts are frequency dependent (Schleifer et al., 2002). The real part σ' is associated with the conduction of electrical charges whose direction is in phase with the applied electric field E. The imaginary part σ'' is related to the displacement currents that are phase-shifted by 90° with respect to the applied electric field.

As a complex quantity the conductivity can also in terms of modulus and phase (Eqs.s. 4 and 5).

Modulus:

$$|\sigma^{*}(\omega)| = \sqrt{(\sigma'(\omega))^2 + (\sigma''(\omega))^2} \tag{4}$$

and phase:

$$\varphi(\omega) = \text{arctg}\left(\frac{\sigma''(\omega)}{\sigma'(\omega)}\right) \tag{5}$$

The phase represents the phase shift between the injected current signal and the measured voltage caused by polarization effects. Classical spectral induced polarization (SIP) instruments measure these two last spectral quantities. We used Lippmann Geophysical instrument (IP Earth Resistivity Meters 4 point light 10 W) during laboratory experiments. It allows investigating polarization effect in the 0.26–25 Hz frequency range, composed of discrete values according to an octave scale. Compared to the other instrument design to study SIP, which frequency typically varies from 10^{-3} Hz to 10^{3} Hz, the frequency range of our study is reduced. Since Martin (2012) and Schleifer et al. (2002) relaxation frequency is located at respectively 0.02 Hz and 7 Hz, we expected a response with frequencies lower than 25 Hz. It was therefore relevant and less time consuming to use the Lippmann device instrument to assess the root polarization effect. For field experiment we used a Terrameter SAS 4000 which performed time domain induced polarization measurements. An alternating field in the form of intervals of current ON and OFF was applied. The frequency range depended on the time duration of injection. Florsch et al. (2011) estimated covered frequencies between 0.25 and 64 Hz. In this case the measure is a time-domain quantity corresponding to the transient decay of the voltage when the transmission is switched OFF and is called chargeability, defined as follow:

$$M_{t_i t_{i+1}} = \frac{1}{V_0}\int_{t_i}^{t_{i+1}} V(t)dt \tag{6}$$

where V(t) is the decaying voltage, t_i and t_{i+1} are the start and the stop time of the interval, and V_0 is the voltage measured before the current is turned off. The time domain chargeability is measured in milliseconds (ms). The full integration on the entire interval t_0 and t_{end}, one often refers to a so-called 'total chargeability'(Florsch et al., 2011).

2.1.1. Data validation and inversion process

We worked on a controlled experimental device designed to perform measurements on a homogeneous soil. Therefore only the presence of buried roots could produce an anomaly of electrical signal. For the field experiment, the interpretation of our results is robust thanks to the accurate location of the roots as a result of ground excavation. Resistivity anomaly ranges obtained could be compared with the resistivity of the root zones in the literature.

In this article data were interpreted after inversion process with Res2Dinv©. Before inversion, we checked all the decay curves and eliminated incoherent points (essentially negative chargeabilities presenting no continuity with neighboring points). Resistivity and IP were inversed concurrently. We choose carefully proper inversion parameters to experimental conditions including few measuring points and small inter-electrode distances. Therefore we selected a suitable mesh and allowed the number of node block to exceed datum points. We choose to reduce effect of side blocks. All inversions presented a relative change in RMS error lower than 5%.

2.2. Laboratory experiment

2.2.1. Data acquisition

During laboratory experiments, we performed electrical measurements to study the IP response at different levels of soil water content. During all the experiment, air temperature was maintained at 23.5 °C and air humidity at approximately 38%.

The methodology used in this study was proposed by Florsch et al. (2011) and Zanetti et al. (2011a, 2011b). Measurements were performed at the soil surface in plastic containers. The control container (A) (length 37 cm, height 28 cm) was filled only with 20 cm of soil while in a similar container (B) a root sample (diameter 4 cm length 20 cm) was buried at 6 cm in depth (Fig. 1). Value of geometric factor (K = 0.37, for 10 cm spacing) has been determined from modeling with finite element software COMSOL®. The root sample was placed

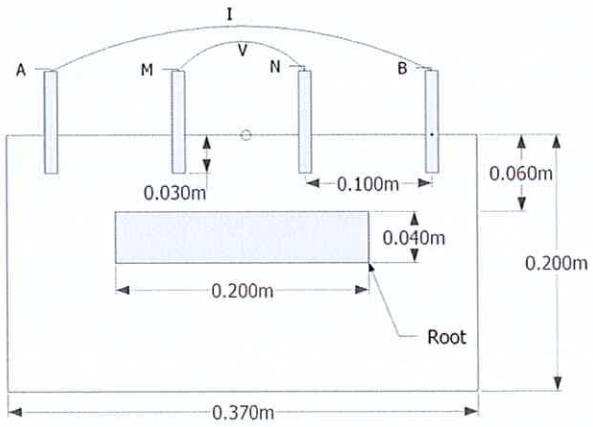

Fig. 1. Sketch of the laboratory setup. A cylindrical root sample is buried in the tank filled with clayey silt soil. Stainless steel current and potential electrodes are placed at the surface of the tank.

in horizontal position and thus was integrated in radial direction, so that results could be compared with previous studies. It also represented a usual situation of running roots in earth dikes (roots growing horizontally). A poplar (*Populus alba*) root sample, freshly collected in the field, was used for this experiment. It was stored in a dark and cool room into a plastic bag to preserve its humidity and fresh weight until the measures. It was intact, displaying two layers, a thin bark and a homogeneous inner wood.

Here, soil is considered as a background and is supposed to be a less polarizable medium than the root. We represented relative differences between a control tank and one containing a root. Initial conditions of experiments are discussed more in detail in Section 2.2.2.

Measurements were conducted from a quadrupole of stainless steel electrode. A Wenner configuration (AMNB) of electrodes was used with constant spacing between each electrode. Thus, measured point is located in the middle of the tank. We choose to work with stainless steel electrodes, first to be able to use them also in the field, then to avoid the contamination of the soil by the chemical solution contained in home-made electrodes. Moreover, such electrodes with a small diameter (0.6 cm) can be considered punctual electrodes (Kruschwitz et al., 2012).

The measure of the potential is less stable in time with polarizable electrodes (stainless steel) than with non-polarizable (Cu/CuSO4) as described by Abdulsamad et al. (2016) In Press. Nevertheless, in our case, it was not a problem for a number of reasons. First, results are presented with relative (and not absolute) variations between a control and a tank containing a root. Secondly, since the quadripole is moved (carefully to always keep the same electrodes positions) between the two tanks, the same electrodes are used between the two tanks and thus the same additional derive (if existing) is applied to the measure. Lastly, visually no oxydo-reduction processes happened between the electrodes and the medium and electrodes remains intact without corrosion.

The result of a measure corresponds to the mean of 30 stacks with a relative difference between two stacks of 0.1% on the phase term (approximately corresponding to a resolution of $\Delta\varphi = 0.2$ mrad at 25 Hz). The electrodes were fixed on a device to accurately fix their position in the tank and their spacing intervals. The depth of investigation depends on electrodes spacing (Dx). Two spacing Dx = 5 and 10 cm were used to check the homogeneity of the drying with time. Although we are quite far from semi-infinite homogenous medium conditions, the effective depth, based on analytical relationship (Edwards and Hillel, 1977), was z = 3.21 and 5.19 cm, respectively for Dx = 5 and Dx = 10 cm. The root sample which top was lying at 6 cm depth (roof) is fully integrated by Dx = 10 cm electrode configuration (Fig. 1). Effective depth was used only for reference to ensure that the root was well enlightened by the electric field at the injection of current knowing that investigation depth changes depending on soil water content. IP measurements were conducted each day during 25 days along with soil water content.

2.2.2. Control of the evolution of the water content

In order to assess the influence of tap water (50 mS/m) content in both tanks A and B, we first saturated the soil (top filling and we waited a few hours to allow water penetration). Using a TDR probe (Time Domain Reflectometry, with a WET-2-Sensor DeltaT Devices) the values of water content at soil surface were controlled before each IP sounding. The measurements were repeated each day to study the evolution of the signal with the decrease of water content of the soil. Surface measures were stacked spatially and repeated in order to control accurately the homogeneity of water content variations in both tanks. To give the absolute water content level, TDR probe have to be first calibrated for the concerned type of soil. In this case we were only interested in the relative variations of water content between the two containers with time (Fig. 2) and a precise calibration was not necessary.

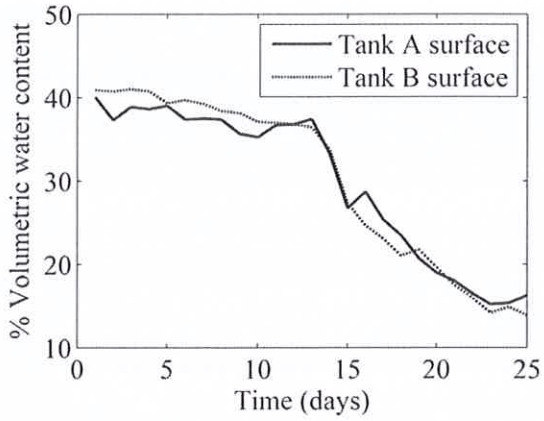

Fig. 2. Trend of the decrease of water content over time during the laboratory experiment: in the control tank with only bare soil (A, plain line) as well as in the tank including a root (B, dash line).

The decrease of water content with the time could be attributed to the drying by evaporation and not to water absorption by the freshly cut root which was saturated by sap. Its trend was similar for both tanks. It allowed us to consider that the electrical investigation was performed in the same conditions for water content and that only the root affected the measured signal.

2.3. Field experiment

2.3.1. Site description

The study site is a grassland located in Aix-en-Provence, in Southern France (N43°31′24.0″N, E5°30′42.0″E). The climate is Mediterranean and is characterized by hot and dry summers and mild wet winters. A weather station is available nearby (200 m) and supplies information on precipitations and temperature.

2.3.2. Experimental design methodology

As the natural soil was not homogeneous, an experimental device with controlled conditions was established. Trees (1 year-old poplars) were planted in large holes (1 m in depth, 1 × 2 m wide) filled with the same homogeneous material than the two containers of the laboratory experiment. The position of each existing coarse root (orientation, depth) was mapped during plantation. Poplars (*Populus alba*) were chosen because they are among the most common species on dikes, they grow fast and generally develop long coarse roots.

One year after plantation, we selected a 320 cm high tree which initial root system was composed of superficial primary coarse roots. In a first step, roots were carefully freed from the material in the first decimeters of soil and a 1-square meter grid with a 5 cm square mesh was laid out (Fig. 3a).

Then the roots were progressively buried again with the same soil, a photo being taken for three different depths respectively z = −35, −10 and −5 cm. These three images were analyzed with a Matlab® program which consists in picking each root in corresponding grid elements and computing a density map. A 10 cm grid was chosen for the final density map, by merging the 5 cm elementary elements, corresponding of the minimum spacing between electrodes in the field. The complex resistivity measurements were positioned with exactly the same grid.

2.3.2.1. Data acquisition. Considering root distribution (Fig. 3), induced polarization measurements were performed along two profiles perpendicular to the main roots. On each profile, the measurements were carried out with 12 stainless steel electrodes, 10 cm spaced. This grid spacing was chosen as a compromise between the spatial resolution adapted to root position in the soil and measurement duration (Fig. 4b).

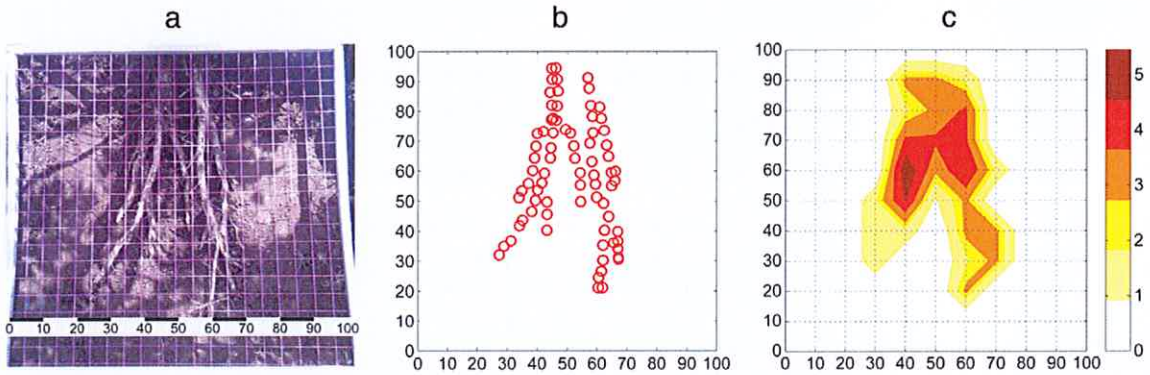

Fig. 3. Root distribution and density in the soil. (a) survey area with roots appearing under the grid (ruler unit in cm) ; (b) root presence picked in elementary grid meshes; (c) roots density computed per mesh. The mesh size corresponds to the minimum distance between electrodes.

Arrays were implemented on a Terrameter SAS 4000 (ABEM instruments). The number of repetitions of the injection cycle performed for each quadrupole depended on data variability but was at least two. Current ON duration was set at 3 s for all experiments, approximately three times longer than the characteristic time constant equal or more than 1 Hz in order to avoid any cumulative effects. The voltage was integrated over six times intervals. The total integration time was set at 3200 ms covering the transient decay of the voltage when the transmitted current was turn off. The first interval started after 10 ms corresponding to the initial time delay. IP measurements used a Wenner-Schlumberger configuration implemented following the recommendation of Dahlin et al. (2013) i.e. not measuring on the same electrode the potential directly after an injection to prevent electrode polarization (as with a dipole-dipole configuration). A root in a soil is a 3D heterogeneity located at shallow depth in all directions (angle, dip) which requires a good vertical and horizontal resolution. Therefore, electrode configuration must allow the best compromise between vertical and horizontal resolution, but also works well for investigations at shallow depths and be sensitive to heterogeneities in 3D. In this sense, by definition Wenner-Schlumberger configuration seems to be the most adapted configuration.

2.3.3. Mapping by monitoring root water uptake: measurement strategy

Simultaneously on the same device, we monitored the evolution of the IP response with time. We hypothesized that biological processes at the interface between roots and soil (root water uptake changing soil water content) could help localizing roots. We first tested the repeatability of measures to set a confidence level of the observed variability, related to instrumental accuracy. Monitoring started in August 5th 2014 following a 65 mm rain event and lasted 3 days. During the two previous weeks, there was no rainfall at the site, and the mean temperature during the day was 25 °C. No watering was provided to trees so that they were under strong water stress. To assess the mean volumetric water content evolution at soil surface, TDR probes were placed at both ends and in the middle of each profile (Fig. 4) data being collected three times a day.

In the case of a tree in field conditions, daily variations in water content and IP response mainly depend on temperature and tree physiology, particularly sap flows (Burgess et al., 2000). According to Boaga et al. (2013) and Doussan et al. (2006) weekly variations associated with the dynamics of water absorption by tree roots are expected. We investigated these spatial and temporal soil moisture changes following the methods proposed by Garré et al. (2011) and Werban et al. (2008). The temperature was measured daily at the same time as IP investigations (9h00 A.M.).

3. Results and discussion

3.1. Laboratory experiment: water content and root discrimination

In the laboratory experiment, very slight differences on complex resistivity were found between the tank with bare soil and the tank

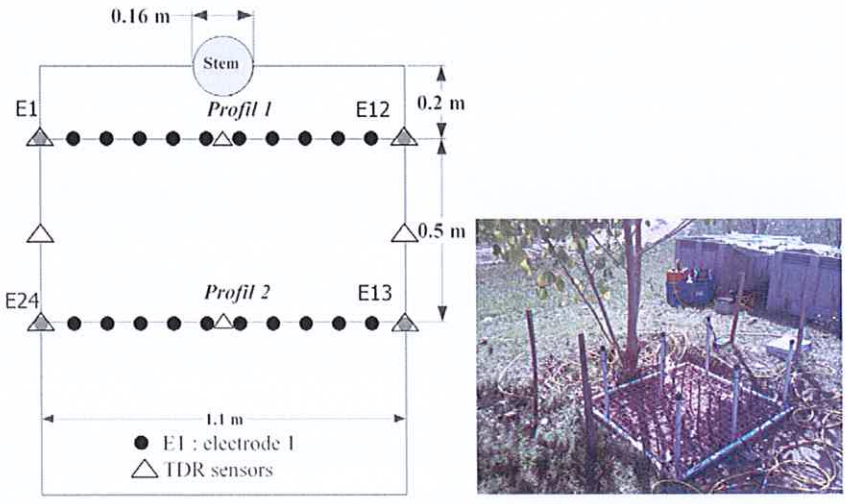

Fig. 4. Square of network of investigation; positions of the two profiles composed of 12 stainless steel electrodes each. Position of temperature and TDR sensors.

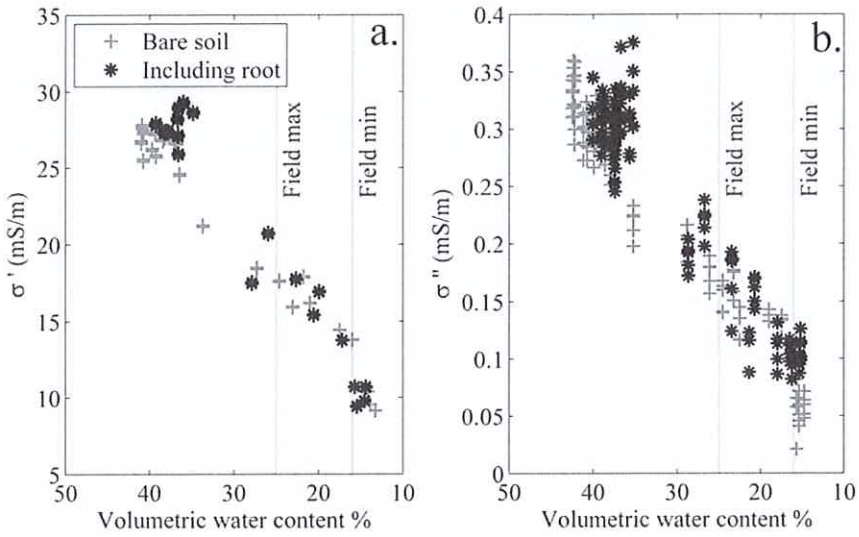

Fig. 5. Evolution of the real part and the imaginary part of conductivity with the decrease of water content (for 10 cm spacing). Black stars represent measurements in the tank including the root, gray crosses in the bare soil. All frequencies from 0.26 to 25 Hz are shown for the imaginary part. Vertical lines show the limits of water content in the field experiment.

containing the root with 10 cm spacing between electrodes. Fig. 5 shows that both real and imaginary parts of conductivity were affected by variations of soil water content (θ). Typically the electrical conductivity decreased with the decrease of water content, ranging between 27 and 14 mS/m for respectively $\theta = 40\%$ and $\theta = 18\%$. The phase term was also clearly dependent on water content as, in both tanks, the phase decreased with soil drying.

The high water content corresponds to the beginning of the experiment. Initial conditions are not relevant for interpretation because the system is still not stable. Water kinetics probably differs between the two tanks due to the presence of the root. For water contents under 17%, differences reached 5.10^{-1} mS/m for the imaginary part. From 36 to 21% of water content, no significant differences were found. The same conclusions may be drawn from Fig. 6, showing that: (i) there is no visible frequency dependency on the real part of conductivity whatever the water content level (36, 21 and 15%) and the real conductivity of the tank with a root is higher than the control tank; (ii) for the imaginary part there is a peak corresponding to the relaxation frequency around 0.52 Hz whatever the tanks. Maximum differences between tanks were found at different frequencies depending on soil water content.

No differences between tanks were found with the five centimeter spacing, (maximum differences $\sigma' = 1.1$ mS/m and $\sigma'' = 7.4.10^{-2}$ mS/m). In this case, current density at the depth of the root was too weak to observe a significant response. This observation confirmed the idea that variations observed with 10 cm spacing electrodes could be attributed to the root. Buried root seems to increase real conductivity because of the higher conductivity of the freshly cut root

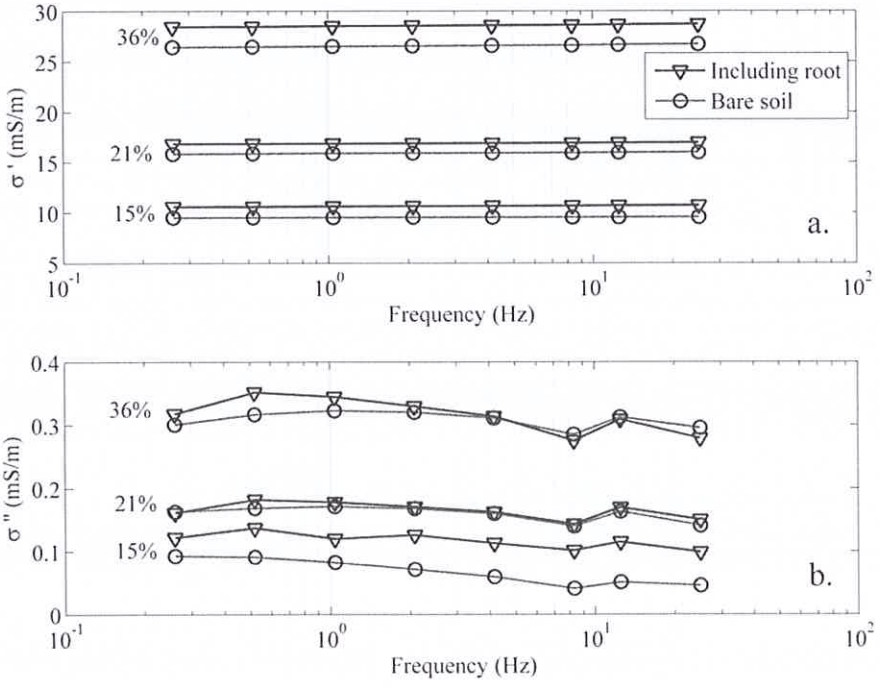

Fig. 6. Evolution of conductivity with frequency and comparison between tank A (bare soil) and tank B (with root) for the real part (6a) and the imaginary part (6b) of the conductivity during soil drying at three levels of water content.

which presented a thin layer of bark and no dead wood and is integrated longitudinally. Finally the root seems to increase the integral conductivity of the ground. Then, the laboratory experiments showed that buried roots samples could act on complex resistivity measurement. The trend of the real part of conductivity was consistent with Archie's Law and existing literature (Ghorbani et al., 2009). For the imaginary part of conductivity we clearly showed that there is a competition between mechanisms induced by roots and soil, whose dominance depends on soil water content. For dry soils ($\theta < 17\%$), which is common in the field, polarization amplitude appears to be significantly higher for root than for soil even if very slightly. The water content of the buried root sample may vary slower than soil humidity during the drying phase, facilitating polarization effects (Martin, 2012). The maximum conductivity ratio between measurements with and without buried root samples for the imaginary part of conductivity was around 1.77 ($\theta = 15\%$). This is consistent with results obtained by Zanetti et al. (2011a, 2011b): a mean increase close to 1.7 of the global imaginary part of conductivity in presence of a buried root sample was observed compared to soil alone. Finally roots polarization effects were observed at low frequency (<25 Hz), which seems relevant and suitable for time domain instruments in the field.

3.2. Maps of spatial variability in the field

A good correlation was obtained, for both sections, between the root density index and respectively a high positive anomaly of resistivity and a negative anomaly of chargeability (Fig. 7A). Some artifacts due to the inversion process appeared on the edge of sections. The global

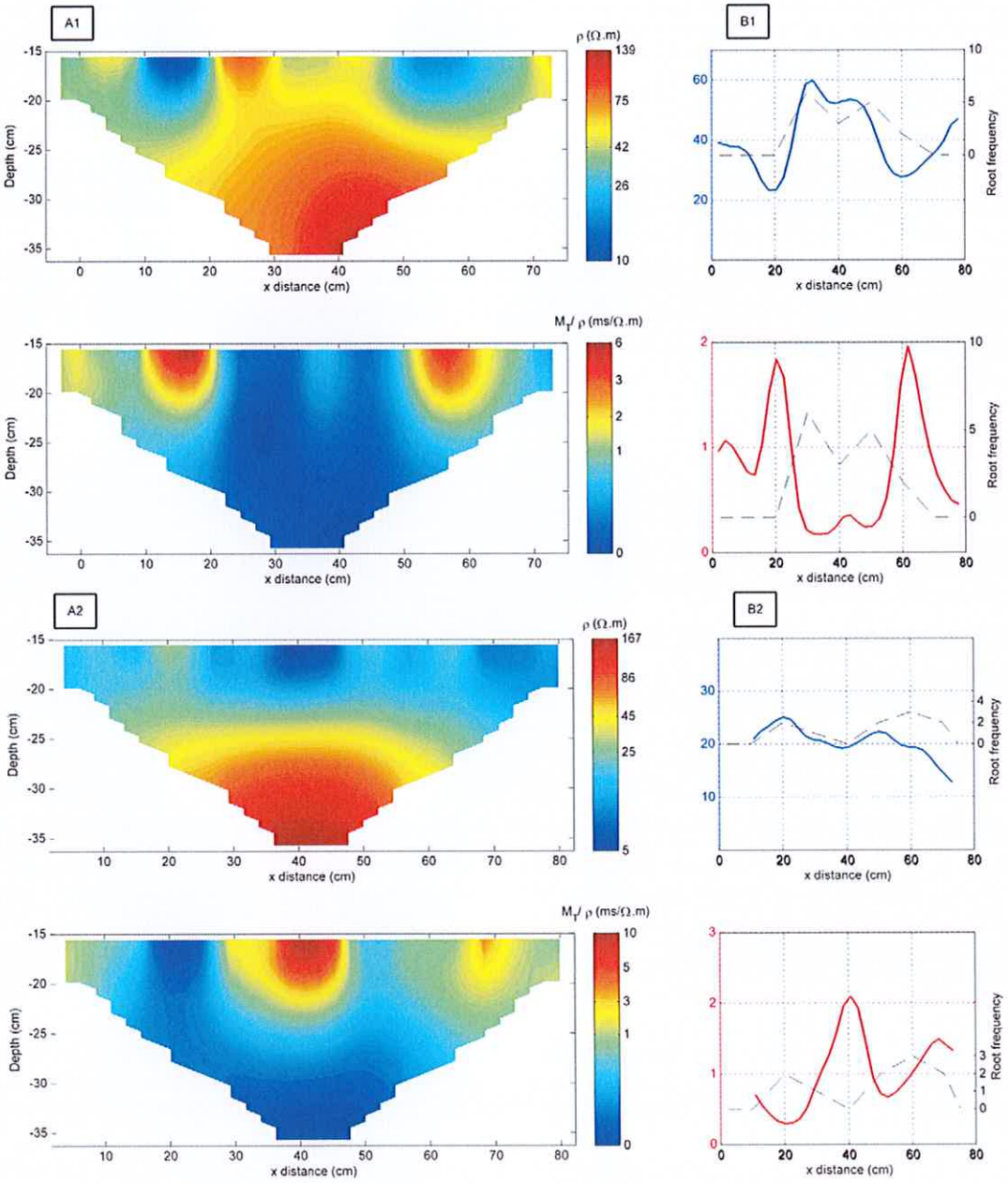

Fig. 7. Resistivity and normalized chargeability inverted sections obtained the first day August 6th with 25% of water content. A: inverted amplitude (Ω·m) (in log scale) and global normalized chargeability (ms/Ω·m) for the two sections: A1–20 cm from the trunk and A2–70 cm from the trunk. B: superposition of root frequency (in dotted line) and respectively resistivity and normalized chargeability profiles extracted at a depth of 25 cm from corresponding plane of panel A (In plain blue lines: amplitude of inverted resistivity—In plain red lines: amplitude of global normalized chargeability).

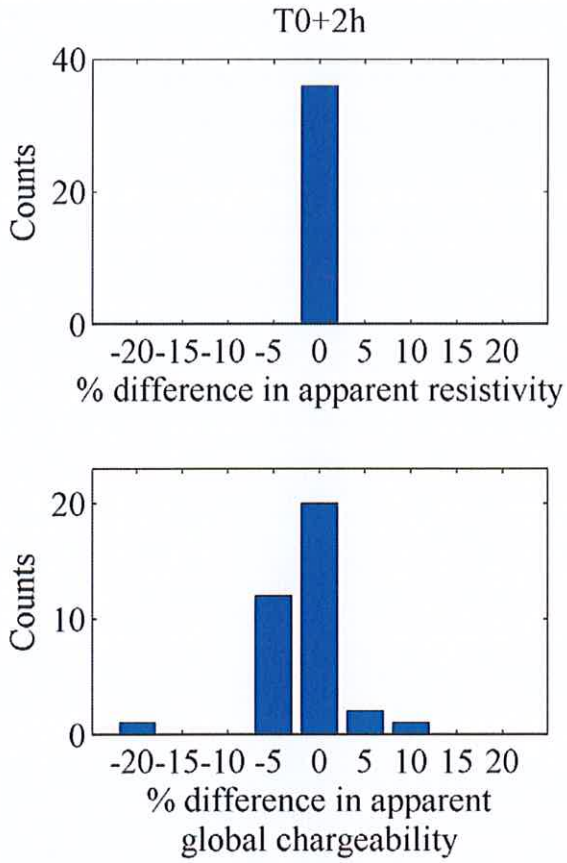

Fig. 8. Histograms showing the percentage of differences with initial measurement (T0) of all apparent data points section 1 for apparent resistivity T0 + 2 h and global apparent chargeability T0 + 2 h.

chargeability was strongly and inversely correlated with resistivity. Fig. 7B shows the excellent fit between root frequency and both resistivity and chargeability in a profile at 25 cm depth, corresponding to the maximum coarse root density. We computed normalized chargeability to free it from variation of resistivity due to the different ground water contents.

The spatial accuracy of the method was sufficient to display two peaks of resistivity and chargeability corresponding to 2 sets of main roots close to each other, and show that roots were diverging progressively with the distance to the trunk (Fig. 3). Spatial variations in resistivity are observed in Fig. 7, and discussed in Section 3.3 as a contribution to the interpretation of temporal variations.

3.3. Mapping by monitoring root water uptake: temporal evolution

3.3.1. Repeatability of the measures

The method proposed by Fiandaca et al. (2013) was used to test the reliability of measures. A second series of measures was obtained 2 h after the first one at the beginning of the experiment. The confidence interval was set at 5%, for resistivity and 7% for chargeability (Fig. 8) as the range containing 95% of the relative differences between the two series. A third set of measures 4 h after the beginning showed larger and numerous variations from the beginning which may indicate a visible effect of biological activity.

3.3.2. Temporal variations

The resistivity showed only positive variations during the monitoring experiment. Conversely, variations of chargeability were mainly negative with a few exceptions (14% of points + 20% of relative changes). These exceptions could be related spatially to the potential effects of root activity, which is supposed to increase the whole chargeability when drying the soil as shown in the laboratory experiment (Fig. 6): with soil drying, the relatively weight of roots compared to soil is increasing in terms of polarization effects.

Spatio-temporal differences appeared between sections at initial time (August, 06) and respectively one and two days later (Figs. 9 and 10).

From the first day, subsequent to a decrease of approximately 6% of superficial water content, we observed: (i) on one hand approximately a 5 ms decrease of the global chargeability in the non-root zone, and (ii) on the other hand, simultaneously, a slight global chargeability increase near the roots. The same trend was observed for next days with less intensity. Although we clearly observed two opposite directions of the response for soil and roots, parasite signal appeared, especially for section 2 (Fig. 7A2) where roots are located more in depth, thus variations of chargeability with soil drying did not match roots density as well as total chargeability at initial time.

Excavation and mapping of the tree root system, and comparison with the measured values, allowed us to interpret anomalies with a good spatial accuracy. In addition, the verification of the confidence intervals for resistivity and chargeability values showed that variations recorded during monitoring experiments were significant. Resistivity is easier to measure since chargeability is a weak phenomenon with a low ratio signal/noise. Chargeability is the result of the combination of the effects of roots and soil for the selected frequency. Nevertheless roots are embedded in soil and, in this experiment as well as more generally, represent only a small proportion of the studied soil section. During the first day of field monitoring ($\theta = 25\%$), roots appeared logically as a strong positive anomaly of resistivity (al Hagrey, 2007). We deal with a homogeneous soil texture and an important root density at low depth which are ideal conditions to detect an anomaly of resistivity. But we obtained unexpected results since root zone did not increase

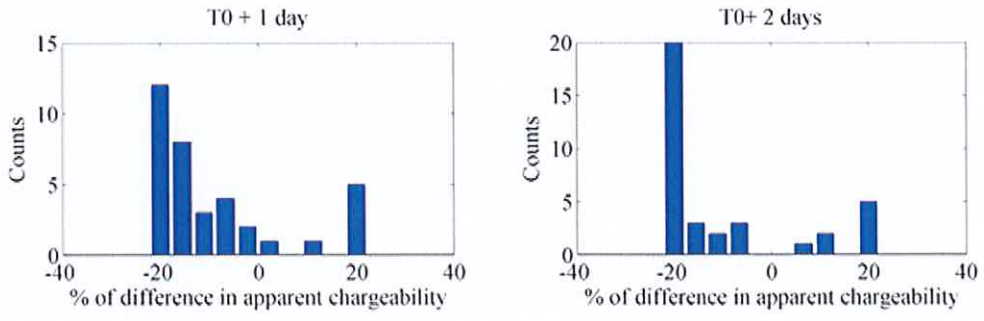

Fig. 9. Histograms showing the evolution of global trend of all data points of section 1 measuring during the tomography measurement 1 day (left) and 2 days (right) after reference measurement.

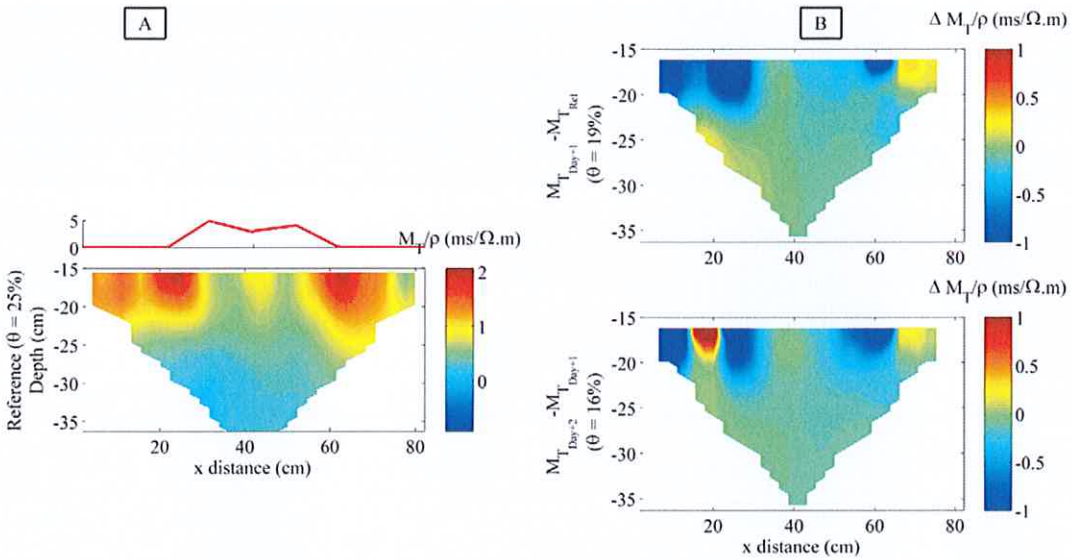

Fig. 10. Section of normalized chargeability; panel a: reference pseudo-section (August 06th) of section 1 displaying also root frequency at 25 cm depth (above); panel b: relative differences between day i + 1 and day i.

the whole chargeability and appeared as a negative anomaly. The strong anomaly of resistivity at the initial time is the consequence of mainly two parameters: a high root mass density associated with lower soil water content than elsewhere in the profile. It means that at the initial time, the section was not homogenous in water content. Soil was dryer in root zone, due to water uptake by roots before watering. Watering by rain progressively rebalanced soil water content. This may explain that even if root mass density should increase the whole chargeability, initial water content is preponderant on the response of chargeability. As the soil was decompacted when removed around the roots to map them, but not at the very border of the plot, some effects of soil compaction may affect IP signal at plot boundary after inversion (Fig. 10), as soil compaction act on pore space (Schleifer et al., 2002). Due to a higher soil compaction and to potential water flows from outside the plot, the decrease of water content may logically be slower at plot border, consistently with the response to IP signal. Compared to laboratory experiment, measurement of global root system integrates also thin roots which contribute to the response of polarization (Kemna et al., 2011). All previously cited studies dealing with frequency dependency of roots sample used SIP instruments; conversely during field experiment we investigated time domain induced polarization. Acquisition parameter settings and particularly injection time (Time ON = 3 s) seem essential to limit the overlapping in the response of soil and roots. Nevertheless, transition from frequency to temporal is complex and the choice of TON = 3 s may not be optimal for roots excitation. Thereby we should probably obtain another chargeability map when time duration is changing. The water content variations are studied here as a parameter that can provide useful information on the location of root zones: root water uptake leads to a hydraulic conductivity drop between the bulk soil and the soil–root interface (Schröder et al., 2009). With the drying of the soil, the chargeability section tends more and more to look like the resistivity section. Other variations disturbing the interpretation in the field study may be attributed to other variations in water content, either by evaporation at soil surface (differences in shading by tree branches) or by water gravity and capillarity flows into the ground from the surroundings.

4. Conclusion and prospects

This paper aims at adding induced polarization to the classical resistivity concept in order to map roots systems in the soil. The ability to detect the roots including polarization effects was highly related to root mass density and soil water content, which both affect polarization. The laboratory experiment showed a slight anomaly of complex resistivity in presence of a buried root sample, mainly at low water content. The field experiment demonstrated that, unexpectedly, resistivity and chargeability at low frequency were inversely correlated for high water contents, even if root mass density was high, suggesting a preponderant effect of root activity on soil hydric status in the response. The evolution of soil water content due to root uptake brought useful information to locate them. However the resolution of the method needs to be improved to map roots accurately. To conclude, it appears that polarization of roots increases the whole chargeability in dry loamy soils. Additional investigations are necessary for a better understanding of the frequency dependence of roots sample, to find a frequency range less affected by loamy soil polarization, and to adapt the method and parameters to other soil types and deeper roots. Ongoing work includes spectral induced polarization (SIP) to investigate soil and roots polarization response to multiple-frequency and particularly at very low frequencies.

Acknowledgment

This research is a contribution to the Labex OTMed (No ANR-11-LABX-0061) funded by the (Investissements d'Avenir) program of the French National Research Agency through the A*MIDEX project (No ANR-11-IDEX-0001-02) and was also supported by IRSTEA.

References

Abdulsamad, F., Florsch, N., Schmutz, M., Camerlynck, C., 2016. Assessing the high frequency behavior of non-polarizable electrodes for spectral induced polarization measurements. J. Appl. Geophys. 135, 449–455.

al Hagrey, S.A., 2007. Geophysical imaging of root-zone, trunk, and moisture heterogeneity. J. Exp. Bot. 58, 839–854. http://dx.doi.org/10.1093/jxb/erl237.

Amato, M., Basso, B., Celano, G., Bitella, G., Morelli, G., Rossi, R., 2008. In situ detection of tree root distribution and biomass by multi-electrode resistivity imaging. Tree Physiol. 28, 1441–1448. http://dx.doi.org/10.1093/treephys/28.10.1441.

Amato, M., Bitella, G., Rossi, R., Gómez, J.A., Lovelli, S., Gomes, J.J.F., 2009. Multi-electrode 3D resistivity imaging of alfalfa root zone. Eur. J. Agron. 31, 213–222. http://dx.doi.org/10.1016/j.eja.2009.08.005.

Archie, 1942. The electrical resistivity log as an aid in determining some reservoir characteristics. I. Pet. Technol. 5.

Aulen, M., Shipley, B., 2012. Non-destructive estimation of root mass using electrical capacitance on ten herbaceous species. Plant Soil 355, 41–49. http://dx.doi.org/10.1007/s11104-011-1077-3.

Bambara, G., Curt, C., Vennetier, M., Mériaux, P., Zanetti, C., Vanloot, P., 2013. Characterization of woody roots located in dikes by near-infrared spectroscopy and chemometrics. Presented at the ICNIRS 2013 16th International Conference on Near Infrared Spectroscopy, p. 274.

Boaga, J., Rossi, M., Cassiani, G., 2013. Monitoring soil–plant interactions in an apple orchard using 3D electrical resistivity tomography. Procedia Environ. Sci. 19, 394–402. http://dx.doi.org/10.1016/j.proenv.2013.06.045.

Burgess, S.S.O., Adams, M.A., Bleby, T.M., 2000. Measurement of sap flow in roots of woody plants: a commentary. Tree Physiol. 20, 909–913. http://dx.doi.org/10.1093/treephys/20.13.909.

Corcoran, M.K., Gray, D.H., Biedenharn, D.S., Little, C.D., Leech, J.R., Pinkard, F., Bailey, P., Lee, L.T., 2010. Literature Review-Vegetation on Levees (DTIC Document).

Dahlin, T., Dalsegg, E., Sandström, T., 2013. Data quality quantification for time domain IP data acquired along a planned tunnel near Oslo, Norway. Procs. Near Surface Geoscience 2013.

Deroo, L., Fry, J.-J., 2014. Projet National ERINOH - Erosion interne - Approches et besoins en matière d'ingénierie (Rapport de recherche No. LC/10/ERI/68).

Doussan, C., Pierret, A., Garrigues, E., Pagès, L., 2006. Water uptake by plant roots: II – modelling of water transfer in the soil root-system with explicit account of flow within the root system – comparison with experiments. Plant Soil 283, 99–117. http://dx.doi.org/10.1007/s11104-004-7904-z.

Edwards, J.T., Hillel, A.J., 1977. The electrical resistivity of G. P. zones. Philos. Mag. 35, 1221–1229. http://dx.doi.org/10.1080/14786437708232948.

Fiandaca, G., Ramm, J., Binley, A., Gazoty, A., Christiansen, A.V., Auken, E., 2013. Resolving spectral information from time domain induced polarization data through 2-D inversion. Geophys. J. Int. 192, 631–646. http://dx.doi.org/10.1093/gji/ggs060.

Florsch, N., Llubes, M., Téreygeol, F., Ghorbani, A., Roblet, P., 2011. Quantification of slag heap volumes and masses through the use of induced polarization: application to the Castel-Minier site. J. Archaeol. Sc. 38, 438–451. http://dx.doi.org/10.1016/j.jas.2010.09.027.

Foster, M., Fell, R., Spannagle, M., 2000. The statistics of embankment dam failures and accidents. Can. Geotech. J. 37, 1000–1024. http://dx.doi.org/10.1139/t00-030.

Garré, S., Javaux, M., Vanderborght, J., Pagès, L., Vereecken, H., 2011. Three-dimensional electrical resistivity tomography to monitor root zone water dynamics. Vadose Zone J. 10, 412–424. http://dx.doi.org/10.2136/vzj2010.0079.

Ghorbani, A., Cosenza, P., Revil, A., Zamora, M., Schmutz, M., Florsch, N., Jougnot, D., 2009. Non-invasive monitoring of water content and textural changes in clay-rocks using spectral induced polarization: a laboratory investigation. Appl. Clay Sci. 43, 493–502. http://dx.doi.org/10.1016/j.clay.2008.12.007.

Gurin, G., Tarasov, A., Ilyin, Y., Titov, K., 2013. Time domain spectral induced polarization of disseminated electronic conductors: laboratory data analysis through the Debye decomposition approach. J. Appl. Geophys. 98, 44–53. http://dx.doi.org/10.1016/j.jappgeo.2013.07.008.

Hagrey, S., Michaelsen, J., 2002. Hydrogeophysical soil study at a drip irrigated orchard, Portugal. Eur. J. Environ. Eng. Geophys. 7, 75–93.

Kemna, A., Binley, A., Ramirez, A., Daily, W., 2000. Complex resistivity tomography for environmental applications. Chem. Eng. J. 77, 11–18. http://dx.doi.org/10.1016/S1385-8947(99)00135-7.

Kemna, A., Pfeifer, J., Weigand, M., Kelter, M., Walter, A., Zimmermann, E., 2011. Imaging Root Systems of Crops Using Spectral Induced Polarization. Zentralinstitut für Elektronik, Pflanzenwissenschaften.

Kruschwitz, S., Niederleithinger, E., Trela, C., Wöstmann, J., 2012. Use of complex resistivity tomography for moisture monitoring in a flooded masonry specimen. J. Infrastruct. Syst. 18, 2–11. http://dx.doi.org/10.1061/(ASCE)IS.1943-555X.0000053.

Mancuso, S., 2011. Measuring Roots: an Updated Approach. Springer.

Martin, T., 2009. Complex resistivity (CR) of wood and standing trees. Proc. of the 16th International Symp. on Nondestructive Testing and Evaluation of Wood, pp. 10–15.

Martin, T., 2012. Complex resistivity measurements on oak. Eur. J. Wood Wood Prod. 70, 45–53. http://dx.doi.org/10.1007/s00107-010-0493-z.

Martin, T., Günther, T., 2013. Complex resistivity tomography (CRT) for fungus detection on standing oak trees. Eur. J. For. Res. http://dx.doi.org/10.1007/s10342-013-0711-4.

Mériaux, P., Vennetier, M., Aigouy, S., Hoonakker, M., Zylberblat, M., 2006. Diagnosis and Management of Plant Growth on Embankment Dams and Dykes. Barcelone. pp. 1–20.

Nadezhdina, N., Ferreira, M.I., Silva, R., Pacheco, C.A., 2008. Seasonal variation of water uptake of a *Quercus suber* tree in Central Portugal. Plant Soil 305, 105–119. http://dx.doi.org/10.1007/s11104-007-9398-y.

Olhoeft, G., 1985. Low-frequency electrical properties. Geophysics 50, 2492–2503.

Preston, G.M., McBride, R.A., Bryan, J., Candido, M., 2004. Estimating root mass in young hybrid poplar trees using the electrical capacitance method. Agrofor. Syst. 60, 305–309. http://dx.doi.org/10.1023/B:AGFO.0000024439.41932.e2.

Schleifer, N., Weller, A., Schneider, S., Junge, A., 2002. Investigation of a Bronze Age plankway by spectral induced polarization. Archaeol. Prospect. 9, 243–253. http://dx.doi.org/10.1002/arp.194.

Schröder, T., Javaux, M., Vanderborght, J., Körfgen, B., Vereecken, H., 2009. Implementation of a microscopic soil–root hydraulic conductivity drop function in a three-dimensional soil–root architecture water transfer model. Vadose Zone J. 8, 783–792.

Sharp, M., Wallis, M., Deniaud, F., Hersch-Burdick, R., Tourment, R., Matheu, E., Seda-Sanabria, Y., Wersching, S., Veylon, G., Durand, E., Smith, P., Forbis, J., Spliethoff, C., 2013. The International Levee Handbook.

Thierry, B., Weller, A., Schleifer, N., Westphal, T., 2001. Polarisation effects of wood. Ext. Abst. für Tagungsband zur EEGS, pp. 44–45 (Birmingham).

Vanderborght, J., Huisman, J.A., Kruk, J., Vereecken, H., 2013. Geophysical methods for field-scale imaging of root zone properties and processes. Soil–Water–Root Processes: Advances in Tomography and Imaging, pp. 247–282.

Vennetier, M., Zanetti, C., Meriaux, P., Mary, B., 2015. Tree root architecture: new insights from a comprehensive study on dikes. Plant Soil 387, 81–101. http://dx.doi.org/10.1007/s11104-014-2272-9.

Weller, A., Frangos, W., Seichter, M., 2000. Three-dimensional inversion of induced polarization data from simulated waste. J. Appl. Geophys. 44, 67–83. http://dx.doi.org/10.1016/S0926-9851(00)00007-0.

Weller, A., Nordsiek, S., Bauerochse, A., 2006. Spectral induced polarisation – a geophysical method for archaeological prospection in peatlands. J. Wetland Archaeol. 6, 105–125. http://dx.doi.org/10.1179/jwa.2006.6.1.105.

Werban, U., Attia al Hagrey, S., Rabbel, W., 2008. Monitoring of root-zone water content in the laboratory by 2D geoelectrical tomography. J. Plant Nutr. Soil Sci. 171, 927–935. http://dx.doi.org/10.1002/jpln.200700145.

Zanetti, C., Vennetier, M., Mériaux, P., Royet, P., Provansal, M., 2011a. Managing woody vegetation on earth dikes: risks assessment and maintenance solutions. Procedia Environ. Sci. 9, 196–200. http://dx.doi.org/10.1016/j.proenv.2011.11.030.

Zanetti, C., Weller, A., Vennetier, M., Mériaux, P., 2011b. Detection of buried tree root samples by using geoelectrical measurements: a laboratory experiment. Plant Soil 339, 273–283. http://dx.doi.org/10.1007/s11104-010-0574-0.

Zanetti, C., Vennetier, M., Mériaux, P., Provansal, M., 2015. Plasticity of tree root system structure in contrasting soil materials and environmental conditions. Plant Soil 387, 21–35. http://dx.doi.org/10.1007/s11104-014-2253-z.

Zenone, T., Morelli, G., Teobaldelli, M., Fischanger, F., Matteucci, M., Sordini, M., Armani, A., Ferrè, C., Chiti, T., Seufert, G., 2008. Preliminary use of ground-penetrating radar and electrical resistivity tomography to study tree roots in pine forests and poplar plantations. Funct. Plant Biol. 35, 1047–1058.